The American Society of Mechanical Engineers

Reprinted From
DE-Vol. 55, Reliability, Stress Analysis, and Failure Prevention
Editor: Richard J. Schaller
Book No. G00816 - 1993

MMC RING FATIGUE AND FRACTURE LIFE PREDICTION: AN ENGINEERING MODEL

Gary R. Halford
Structures Division
NASA Lewis Research Center
Cleveland, Ohio

ABSTRACT

The framework of an engineering creep-fatigue durability model has been adapted for use in estimating the radial static burst pressure and cyclic low-cycle fatigue macro-crack initiation resistance of continuous fiber reinforced (CFR) metal matrix composite (MMC) rings for application at 800 °F. Rings of circumfrentially wrapped SCS6/Ti-15-3 were manufactured by Textron Specialty Metals and burst tested by Pratt & Whitney as a part of a cooperative program with the NASA Lewis Research Center. Fatigue tests have as yet to be performed. The engineering model is based on a 3-D elasto-plastic micromechanics analysis of the tensile-loaded composite architecture. Use is made of the rule of mixtures, strain compatibility, equilibrium, and the stress-strain relationships of the constituents. Knowledge is required of the mechanical and fatigue properties of the matrix and fibers and how the presence of each affects the sharing of imposed stresses and strains. The model addresses specific issues such as residual fabrication stresses, inelastic deformation within the ductile matrix, multiaxial constraint imposed on the matrix, cyclic relaxation of both residual and applied mean stresses in the matrix, fatigue micro-crack initiation and propagation in the matrix, and tensile fracture of both the ductile matrix and the brittle fibers. In the current application of the model, the specific issues were empirically calibrated through use of tensile and tension-tension fatigue coupons that had been subjected to essentially identical loading as the rings.

NOMENCLATURE

Symbols

A	cross-sectional area or classical fatigue ratio, alternating/mean
B	intercept of elastic strainrange - life relations
C	intercept of inelastic strainrange - life relations
C'	intercept of inelastic line for creep-fatigue cycles
CTE	coefficient of thermal expansion
F	inelastic strain fraction
K	cyclic strain-hardening coefficient
L	radial load per shoe
N	number of applied cycles
R	ratio, algebraic minimum to maximum
V	ratio, mean to alternating
MF	multiaxiality factor
TF	triaxiality factor
Δ	range of variable
ϵ	strain
σ	stress
Σ	summation

Subscripts

cc	creep strain in tension, creep strain in compression
cp	creep strain in tension, plastic strain in compression
el	elastic
f	failure with zero mean stress
fm	failure with mean stress
i	micro-crack initiation with zero mean stress
ij	pp, pc, cp, or cc
in	inelastic
L	load
p	micro-crack propagation with zero mean stress
pc	plastic strain in tension, creep strain in compression
pp	plastic strain in tension, plastic strain in compression
t	total
u	ultimate (tensile strength)
y	yield (0.2 percent offset)
ϵ	strain
σ	stress

Superscripts

b	power for elastic strainrange - life relations
c	power for inelastic strainrange - life relations
n	cyclic strain-hardening exponent ($\approx$ b/c)

INTRODUCTION

The framework of an engineering creep-fatigue durability model has recently been presented (Halford et al, 1993) that addresses the key crack initiation and growth issues involved in the high-temperature, low-cycle fatigue (LCF) resistance of [0°] continuous fiber reinforced metal matrix composites (MMCs). Originally proposed for dealing with thermomechanical fatigue (TMF), adaptation to isothermal loading conditions was a relatively simple matter. The model has been used herein to estimate the 800 °F radial static burst pressure and low-cycle fatigue life of cyclically-loaded, continuous-fiber reinforced MMC rings (fibers aligned with the circumfrential, maximum principal stress direction, i.e., [0°]). The program was part of a four year cooperative effort between Pratt & Whitney's Government Engines and Space Propulsion Group and the National Aeronautics and Space Administration's Lewis Research Center. Overall results of that program are the subject of this paper. Several other durability models were developed over the course of the program and have been reported upon by their creators in the other papers comprising this volume.

FRAMEWORK OF THE MODEL

The MMC material was treated as if it were a conventional structural element whose weakest, most highly stressed regions are the likely origins of failure initiation, Fig. 1. As

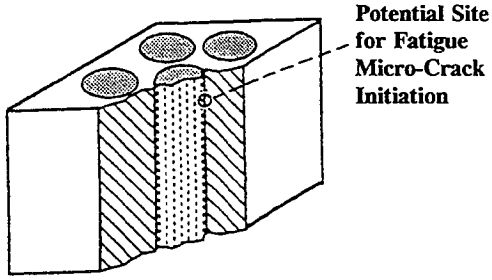

Fig. 1 A Composite Material is a Mini-Structure.

with conventional structures, the durability of an MMC was expected to be governed by localized stress, strain, and temperature conditions, and their variation with time. Micro-mechanical structural analysis techniques were used to calculate local conditions. While the metallic matrix was used as the vehicle for tracking fatigue damage evolution, due consideration was also given to the stress-strain and fracture characteristics of the brittle fibers, and the structural interactions of fiber, interface, and matrix. A representation of these interactions is shown schematically in Fig. 2.

The engineering durability model has three major elements:

1) Creep-fatigue equations reflect both the flow and failure behavior of the *in situ* matrix material. Equations are calibrated from test results of unreinforced matrix material which may differ slightly from its *in situ* counterpart. The measured macro-crack initiation fatigue life (usually defined as complete separation of coupon-sized axial specimen) of the matrix material is apportioned into micro-crack initiation and micro-crack propagation phases.

2) The matrix flow and failure response is altered by the presence of fibers and interfaces. Some of the influences act solely on the micro-crack initiation portion of the matrix fatigue life, others on the micro-crack propagation life while some affect both.

3) The recognition of overriding influences such as a maximum tensile strain limit of brittle fibers that could cause individual fiber fractures and ensuing catastrophic failure of the surrounding matrix.

The matrix material's isothermal creep-fatigue flow and failure behavior is characterized in terms of the Total Strain version of Strainrange Partitioning (TS-SRP) (Saltsman and Halford, 1988a). The term "creep-fatigue" is used since the cycles emphasize creep deformation superimposed on strain-limited fatigue cycling. Since the tests typically are performed on specimens in a laboratory air atmosphere, they are also subject to oxidation. It is tacitly implied that "creep-fatigue" experiments in air produce results that reflect the interactions of all three important failure behavior factors: fatigue, creep, and oxidation.

In addition to documentation of creep-fatigue-oxidation failure characteristics, it is also necessary to establish the cyclic viscoplastic flow behavior of the matrix. The TS-SRP life prediction approach is applicable to any generalized, time-dependent, creep-fatigue cycle. Generality is achieved through the use of existing Unified Viscoplastic Models (Bodner and Partom, 1975; Walker, 1981; Robinson and Swindeman, 1982; Freed, 1988) to represent the flow behavior. On occasion, we have had to resort to simpler, less-general, empirical, power-law relations to document the required cyclic flow behavior (Halford et al, 1991a).

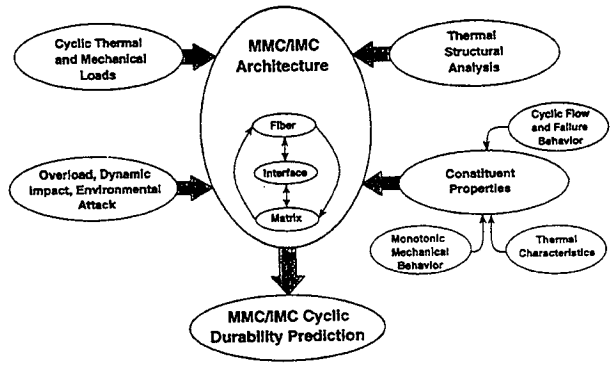

Fig. 2 Framework for Engineering Creep-Fatigue Life Prediction Modeling of MMCs.

Failure Behavior Equations for Matrix

Macro-crack initiation. Once the flow and failure characteristics of the matrix material have been established, the total mechanical strainrange *versus* fatigue life equation can be written for any arbitrary isothermal creep-fatigue cycle. Herein, the definition of the macro-crack initiation life is equal to the fatigue life defined for coupon-sized axial specimens.

Figure 3 graphically displays the total mechanical strainrange *versus* fatigue life relation for matrix material based on the TS-SRP representation. Pertinent equations are shown in the figure. Step-by-step procedures for calibration of the constants in the subject equations are given by Saltsman and Halford, 1988a. The resultant creep-fatigue prediction equation is for the matrix material and is applicable for the specifically stated loading condition, i.e., the isothermal temperature and strain versus time history. Should a significantly different set of loading conditions be imposed, a new set of equation constants are readily calculatable from the already established flow and failure characteristics.

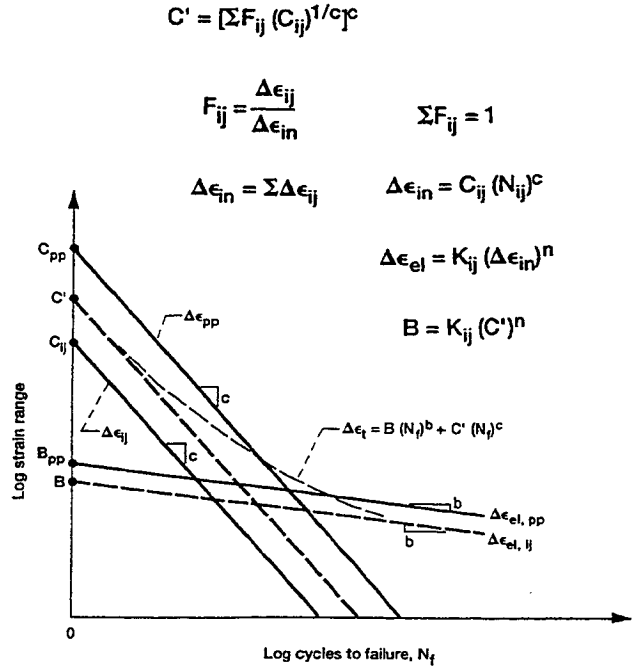

Fig. 3 Creep-Fatigue Life Equations and Strain-Life Curves for Matrix Material. Condensed from Saltsman and Halford, 1988a, (ij = pp, pc, cp, cc).

The life prediction equation shown at this stage represents conditions involving no fibers, no geometric discontinuities (i.e., no stress concentrations), zero mean stress, a uniaxial stress-strain state, and continuously repeated loadings of constant total strainrange, frequency, temperature, etc. Modifications of the equation to deal with specific influencing factors associated with a composite are discussed in the subsequent section. Some of the influences can be described analytically and quantitative computations of the expected effect on TMF life are possible. Other influences are not as yet at the quantifiable stage, and for the meantime will require empiricism and calibration of computations with experimental creep-fatigue results on the composite material.

Some of the influencing factors of the fibers will affect micro-crack initiation more than micro-crack propagation, and vice versa. It is convenient therefore to distinguish, analytically, these two important components of the total macro-crack initiation life.

Approximate equations for the micro-crack initiation and propagation portions of the total fatigue life are given below. First, the total strainrange can be decomposed into its elastic and inelastic strainrange components,

$$\Delta\epsilon_t = \Delta\epsilon_{el} + \Delta\epsilon_{in} \quad (1)$$

Power-law relations between strainrange components and fatigue life (zero mean stress conditions) are commonly observed, i.e.,

$$\Delta\epsilon_{el} = B(N_f)^b, \quad (2)$$

and,

$$\Delta\epsilon_{in} = C(N_f)^c \quad (3)$$

thus, for macro-crack initiation,

$$\Delta\epsilon_t = B(N_f)^b + C(N_f)^c \quad (4)$$

Micro-crack initiation and propagation. Macro-crack initiation fatigue life can be decomposed into micro-crack initiation and micro-crack propagation phases,

$$N_f = N_i + N_p \quad (5)$$

There is widespread acceptance of the notion that micro-cracks initiate very early in low-cycle fatigue (LCF), leaving the vast majority of life to be spent in micro-crack propagation. Furthermore, in high-cycle fatigue, micro-cracks initiate late in life and the micro-crack propagation phase is a small fraction of the total life. Although somewhat arbitrary, it is not unreasonable to assume that:

At a very low life of $N_f = 10$,

$$N_i \approx 0.1N_f \quad (6a)$$
$$N_p \approx 0.9N_f \quad (6b)$$

and, at an arbitrarily high cyclic life of $N_f = 10^7$,

$$N_i \approx 0.9N_f \quad (6c)$$
$$N_p \approx 0.1N_f \quad (6d)$$

Power-law relationships can be written between N_f and N_i and between N_f and N_p using the sets of coordinates of Eqs. (6a) and (6b) and Eqs. (6c) and (6d). That is, $N_f = 10(N_i)^{0.863}$ and $N_f = 0.733(N_p)^{1.19}$. When written in this simple form, the sum of the micro-crack initiation and propagation lives falls short of the total macro-crack initiation life, N_f by about 40% at N_f of 10^4 cycles. At either higher or lower lives, this error diminishes to 0 at 10 and 10^7 cycles to failure. Substituting these relationships into Eq. (4), with b = - 0.12 and c = - 0.60 (Manson, 1965), yields the following approximate relationships.

For micro-crack initiation,

$$\Delta\epsilon_t \approx 0.76\ B\ (N_i)^{-0.1} + 0.25\ C\ (N_i)^{-0.5} \quad (7)$$

For micro-crack propagation,

$$\Delta\epsilon_t \approx 1.04\ B\ (N_p)^{-0.14} + 1.20\ C(N_p)^{-0.7} \quad (8)$$

Influences of Fibers/Interfaces on Matrix Flow and Failure Behavior

The fact that fibers are present in a composite imparts changes in both the flow and failure response of the matrix. A listing of the most significant mechanical influences on the surrounding matrix is given in Table 1. Each factor is identified as to whether it influences the micro-crack initiation or micro-crack propagation phases of the macro-crack initiation life. A few of the influences currently can be handled analytically, others require development. Currently identified influences are discussed below.

TABLE 1 -- Factors associated with fibers mechanically influencing matrix fatigue response.

FACTOR	N_i	N_p
CTE Mismatch Strains	Yes	Yes
Residual (Mean) Stresses	Yes	Yes
Multiaxial Stress State	Yes	Yes
Off-Axis Fibers	Yes	Yes
Internal Stress Concentrations	Yes	No
Multiple Initiation Sites	Yes	Yes
Non-Uniform Spacing	Yes	Yes
Interfacial Layers	Yes	No
Fractured Fibers	Yes	No
Fiber De-bonding	No	Yes
Fiber Crack Retardation	No	Yes
Fiber Bridging	No	Yes

CTE mismatch strains. The CTE mismatch between matrix and fiber causes post-fabrication residual stresses in the MMC. Typically the matrix residual stress is tensile, while the fiber is in compression. For isothermal fatigue at room temperature, the CTE mismatch strain caused by cooling from a fabrication/heat treatment temperature usually produces a detrimental tensile residual stress in the matrix that will act as a mean stress in subsequent fatigue loading provided the residual stress doesn't relax cyclically due to inelasticity in the matrix (or relax via creep at elevated temperatures).

Mean stress effects. Procedures for dealing with mean stresses in strain-based fatigue life models are given by Saltsman and Halford (1988b). They utilize modification (Halford and Nachtigall, 1980) of the Morrow (1968) mean stress approach.

$$(N_{fm})^{-b} = (N_f)^{-b} - V_\sigma \qquad (9)$$

V_σ is the ratio of mean to alternating stress, and is equal to the inverse of the classical fatigue A ratio. For strain-controlled cycles involving detectable amounts of inelasticity, any initially present mean stresses will tend to cyclically relax, numerically reducing the value of V_σ. During creep-fatigue loading, the numerical value of V_σ may be non-zero but is ineffective in altering fatigue in accordance with a transition equation given and discussed by Halford and Nachtigall (1980).

Multiaxiality of stress. Fibers cause multiaxial stress-strain states within the matrix (even though the loading on the unidirectional MMC is uniaxial) as a result of their differing elastic and plastic stress-strain properties, and their differing thermal conductivities and expansion coefficients. Effects on cyclic life due to deviations from uniaxial stress-strain states can be handled by a relatively simple procedure given by Manson and Halford (1976) and Manson and Halford (1977). The multiaxiality factor, MF, is a measure of the degree of hydrostatic stress normalized by the corresponding von Mises effective stress. The MF is used in assessing fatigue life just as a stress concentration factor would be used, i.e., the nominal effective strainrange is multiplied by the MF to obtain the local effective strainrange, which in turn affects the local micro-crack initiation life. The equation for the multiaxial factor is,

$$MF = TF \qquad TF \geq 1 \qquad (10a)$$

$$MF = 1/(2\text{-}TF) \qquad TF \leq 1 \qquad (10b)$$

where,

$$TF = (\sigma_1+\sigma_2+\sigma_3)/(1/\sqrt{2})\sqrt{[(\sigma_1-\sigma_2)^2+(\sigma_1-\sigma_3)^2+(\sigma_2-\sigma_3)^2]} \qquad (10c)$$

and, σ_i = principal stresses (i = 1,2,3)

The multiaxiality factor within the matrix material at the location shown in Fig. 1, for unidirectional loading of a unidirectional fiber layup for the SCS-6/Ti-15-3 MMC system was determined to be only 1.04 (Halford et al, 1989). Multiplying 1.04 times the computed effective strainrange yields the strainrange for entering the matrix total strainrange versus macro-crack initiation life equation. This would give rise to a calculated decrease in fatigue life of only about 10%. Higher multiaxiality factors would give rise to lower fatigue lives.

Off-axis fibers. Relatively small deviations of fiber orientation from [0°] can be responsible for large losses in fatigue resistance. A shift from a 5 degree to a 10 degree off-axis loading has been shown by Hashin and Rotem (1973) to cause a loss of a factor of approximately two in isothermal fatigue strength. The corresponding loss in cyclic lifetime was measurable in terms of multiple orders of magnitude. A 60 degree off-axis loading resulted in a loss of nearly an order of magnitude in fatigue strength.

Internal stress concentrations/multiple initiation sites. An internal micro-stress concentration factor produces higher local internal stresses and strains and promotes earlier micro-crack initiation. Once the micro-crack grew away from the local concentration, however, the concentration effect would diminish and the micro-crack propagation portion of life would be relatively unaffected.

Internal crack initiation at local stress-strain concentrations can occur in MMCs at multiple initiation sites, thus leading to shorter paths for cracks to follow prior to linking together and hastening the macro-fracture of the composite. If micro-crack growth paths are decreased by an average of a factor of two, it would be expected that the micro-propagation phase of life would also decrease by a factor of two.

Non-uniform fiber spacing. Structural analysis can be used to determine the influence of non-uniform fiber spacing on the stress-strain response behavior of the *in situ* matrix. The

alteration of the local stresses and strains will cause corresponding changes in the calculated micro-crack initiation life. Little effect on the micro-crack propagation life would be expected for this influencing factor.

Interfacial layers. Additional examples of using structural analyses to ascertain effects of fibers and interfaces on matrix stress-strain response is found in the work of Jansson and Leckie (1990) and Arnold et al (1990) for assessing the influence of compliant interfacial layers between fibers and matrix. An obvious influence of the rather weak bonding between fiber and matrix (resulting from the low strength of the interfacial layer in the SCS6/titanium system) is to decrease the ability of the fibers to 'bridge' crack faces, i.e., to hold the faces closer together once a crack has formed. The net result is a decreased resistance to crack propagation and a lowered apparent fracture toughness.

Additional influencing factors associated with cracks or de-bonding. Further analytic development of the proposed framework will be required to quantitatively model the impact on micro-crack propagation life of some of the influencing factors not discussed above. Of particular interest are those factors directly associated with micro-cracks within an MMC, i.e., fractured fibers and fiber debonding (the concepts proposed by Chen and Young (1991), among others, offer a promising approach), fiber crack retardation, and fiber bridging (see applicable work of Ghosn et al, 1991). The more highly localized are the stress and strain, the less likely a significant influence will be expected on N_p.

Metallurgical interactions. The presence of distributed non-metallic fibers can influence the metallurgical state of the matrix material. Heat treating of the matrix in the presence of fibers can result in a somewhat different microstructure, yield strength, ultimate tensile strength, ductility, and hardness than obtained by heat treating unreinforced matrix metal (Lerch et al, 1990). This influence will compound the problem of isolating the true cyclic flow and failure behavior of the *in situ* matrix material.

Another crucial factor is the potential for increased internal oxidation of the MMC made possible by the interfacial layers acting as diffusional pipelines within the interior of the MMC. Internal oxidation will dramatically reduce an MMC's TMF resistance by promoting early micro-crack initiation and faster micro-crack propagation.

INFLUENCES OF MATRIX ON FIBERS/INTERFACES

It is also necessary to examine the mechanical influence of the matrix on the response characteristics of the reinforcing fibers. Fibers of primary concern (For example, SCS-6) are elastic and brittle. They fail progressively throughout the fatigue life of the MMC as a result of the continual shedding of tensile stresses from the matrix material as it cyclically deforms. Cyclic relaxation of mean (residual) stresses and strain-hardening or -softening of the matrix results in various scenarios of behavior depending upon the combination of operative conditions. Detailed discussion of various possibilities is given in the next section.

IMPLICATIONS OF MODELING FRAMEWORK TO MMC COUPON TESTS

Some isothermal fatigue coupon results for the SiC/Ti-15-3 MMC system were generated during the NASA/P&WA Cooperative Ring Program. These have been examined in light of the above points of view, and the results extended to the prediction of the radial burst strength and the isothermal low-cycle fatigue life of cyclically loaded rings.

These coupon results, shown in Fig. 4, are for 800 °F with $R_L \approx 0$ and cyclic frequencies ranging between about 0.03 and 0.3 Hz, depending upon strainrange and testing laboratory.

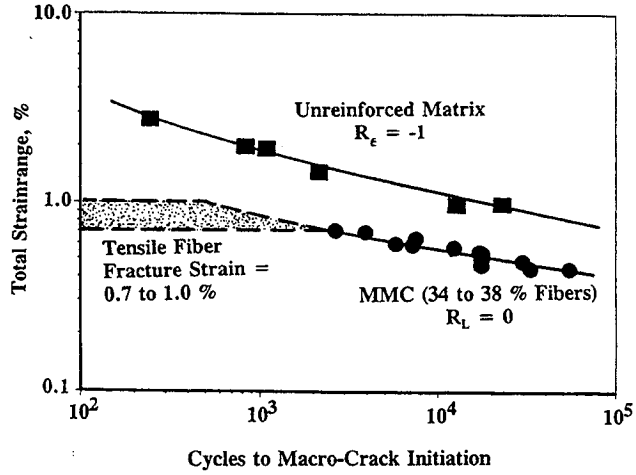

Fig. 4 Comparison of Isothermal Fatigue Resistance of SCS-6/Ti-15-3 MMC (previously unpublished NASA and Pratt & Whitney data) with Ti-15-3 Unreinforced Matrix Material (Gayda et al, 1990).

Fiber volume fractions range from 34 to 38%. The MMC results are compared to isothermal, strain-controlled, R_ϵ = -1, data reported by Gayda et al (1990) for matrix material processed in the same fashion as the composite. Frequencies ranged between 0.03 and 1.0 Hz, and were the highest at the lowest strainranges. Substantially reduced strain fatigue resistance is exhibited by the MMC when compared to the unreinforced matrix. The reduction is a factor of approximately 2 in strainrange for a fixed life, or a factor of about 40 in life for a given strainrange. Among the dozen influential factors previously discussed, few could be responsible for the significantly large loss in fatigue resistance caused by the presence of fibers in the Ti-15-3 matrix. The most pertinent influences are discussed in the following paragraphs.

Any mean stresses in the matrix that may be present due either to the nature of loading or to residual fabrication stresses are expected to cyclically relax to zero for Ti-15-3 at 800 °F. Experimental results supporting this argument have been reported by Gayda et al (1990) for axially loaded

specimens of a 33 volume percent $[0°]_4$ SCS-6/Ti-15-3 MMC. They also generated cyclic strain-controlled data for unreinforced specimens of the matrix material and showed that, for $R_\epsilon = 0$ tests, the initially large tensile mean stress quickly relaxed to zero, i.e., $V_\sigma \rightarrow 0$, resulting in hysteresis loops identical to those for $R_\epsilon = -1$ tests. Thus, from the standpoint of the effect of mean stresses in the matrix, it is not expected that the matrix material would initiate and propagate micro-cracks earlier in the MMC than if fatigued alone.

However, a larger peak tensile stress is experienced by the fibers as they carry a greater portion of the tensile load following relaxation of the matrix tensile mean stresses. Hence, the fibers are forced to operate closer to their peak tensile strain capacity (0.7 to 1.0 %), and the MMC becomes less tolerant of subsequent matrix cracking that will further erode load bearing area and transfer more and more tensile stress (and hence, strain) to the fibers. The cyclic durability resistance of the MMC thusly would be compromised; not by fatigue cracking *per se*, but by the cyclic flow response characteristics of the matrix and the limited strain capacity of the brittle fibers.

Explanation for an additional portion of the discrepancy can be found in the examination of differences in control modes used in the two test series. The MMC fatigue tests used load control and only tensile loads were imposed ($R_L = 0$), whereas the matrix fatigue tests were conducted under completely-reversed strain control ($R_\epsilon = -1$). Had the MMC fatigue tests been conducted with the same range of load, and hence same range of strain with $R_L = -1$ (to keep the results of Fig. 4 more comparable), the peak tensile stress (or strain) experienced by the fibers would have been 50% lower. Consequently, much more extensive matrix fatigue cracks and considerable fiber cracking would had to have occurred before the remaining load carrying fibers were pushed to their peak tensile strain limit. Using this line of reasoning, the MMC specimens could have endured more loading cycles, thus resulting in lives closer to those exhibited by the unreinforced matrix material.

Additional qualitative explanation for the discrepancy is found in the micro-crack propagation portion of cyclic life which can be reduced in the MMC as a result of two important factors. First, in the MMC, cracks can initiate internally and subsequently link, thus reducing cyclic life. Secondly, internal oxidation at 800 °F can occur along the interfaces and any interior cracks. A loss of a factor of 4 in micro-crack propagation life by these means is certainly within the realm of possibility. Furthermore, the micro-crack initiation portion of specimen fatigue life has been observed via fractography by Gayda et (1990) to be essentially bypassed in this MMC system. This is likely due to the nature of the interfacial material and its relatively poor bonding to both fiber and matrix. At a cyclic strainrange giving a life of 10^7 cycles to failure for the unreinforced matrix material, the micro-crack initiation portion is expected to be 90 percent of the total macro-crack initiation life in accordance with Eq. (6c). Thus an additional factor of 10 loss in life can be attributed to the loss of micro-crack initiation life. The two life losses are multiplicative, i.e., 4 x 10 = 40, which is in general agreement with the losses observed in Fig. 4. For the time being, it is not possible to quantify the degree of loss with any confidence in accuracy. A series of strain-controlled, $R_\epsilon = -1$ low-cycle fatigue tests of MMC coupons is planned. The results are expected to provide a better understanding of the causes of the large observed life losses in this MMC material for $R_L = 0$.

APPLICATION OF MODEL FRAMEWORK TO STATIC RING BURST TESTS

Dimensions of each of the three rectangular cross-section rings varied somewhat owing to the manufacturing process. Dimensions of a radial cross-section of Ring No. 1 are shown in Fig. 5. Only the core of the ring was fiber reinforced. Fibers were circumfrentially oriented using a nominal 0.33 fiber volume fraction. The corresponding core dimensions were 0.54" wide, 6.42" OD and 5.57" ID resulting in a radial thickness of about 0.437". As a result of the rather substantial monolithic titanium cladding surrounding the core, the overall fiber volume fraction of a cross section varied from about 0.144 for Ring No. 1 to 0.175 for Ring No. 2. Ring Nos. 2 and 3 had similar appearing cross-sections.

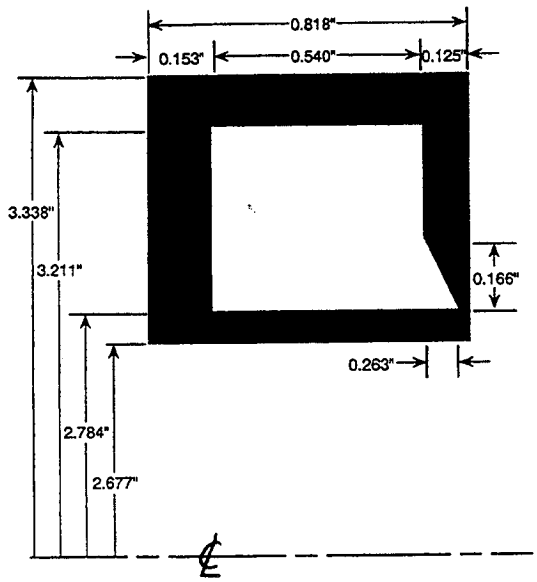

Fig. 5 Cross-Section of Ring No. 1. Core is 0.33 Fiber Volume Fraction Unidirectional SCS-6/Ti-15-3. Solid Cladding is Ti-15-3.

Radial mechanical loading was applied to each ring through 12 equally space and independently loaded shoes. The radial-segmented shoes imparted a 'pressure' loading to the ring's ID surface as shown in Fig. 6. Each shoe was connected to a pinned clevis that was attached, in turn, to a hydraulic cylinder located well beyond the ring OD. The hydraulic cylinders were manifolded to a common hydraulic supply. The net result of this manner of loading was to place the ring in nominally circumfrential tension. However, the radial thickness was sufficient to produce a substantial radial gradient of applied strain with the ID experiencing a strain about 20% greater than the average circumfrential strain along the radial thickness.

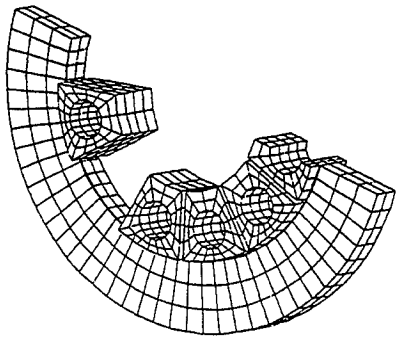

Fig. 6 MMC Ring and Radial Loading Shoes.

This gradient will cause material near the ID to initiate failure. Since the material at the ID is ductile Ti-15-3, failure will not occur there, but more likely will initiate in the brittle SCS-6 fibers that are contained in the core which is located about 0.107" radially beyond the ID. At the location of the first rows of fibers, the circumfrential strain for Ring No. 1 will be only about 13.5% higher than the average. Ring No. 1 was statically burst tested at 800 °F.

It is assumed that burst under static radial loading will commence when the local stress reaches the ultimate tensile strength of the core composite material. The failure initiation location will be at the ID of the core where the local strain (and hence stress for a nominally-elastic, brittle-fiber MMC) is 13.5 % higher than the calculated average circumfrential ring stress. When the core material is at an average stress of 13.5 less than its ultimate tensile strength, the Ti-15-3 cladding material will, on average over its cross-sectional area, be very near its yield strength (higher at the ID, lower at the OD). Equating the internal forces (average circumfrential stresses, σ_{core} and σ_{clad}, times their respective areas, A_{core} and A_{clad}) to the externally applied loads (expressed as a function of the radial load applied per shoe), we arrive at, for Ring No. 1,

$$3.8625\ L = 2[\sigma_{core} \times A_{core} + \sigma_{clad} \times A_{clad}] \qquad (11a)$$

$$3.8625\ L = 0.4716\ \sigma_{core} + 0.6098\ \sigma_{clad} \qquad (11b)$$

At commencement of burst, $\sigma_{core} = (1/1.135)\ \sigma_{u,MMC} = 185.5$ ksi at 800 °F and $\sigma_{clad} = \sigma_{y,Ti\text{-}15\text{-}3} = 122$ ksi at 800 °F. Thus, burst is calculated to occur at a load per shoe, L of 41.9 kips. This corresponds to an average pressure applied to the ring ID of 36.5 ksi.

Experimentally, Ring No. 1 burst at an ID pressure of 27.46 ksi, considerably below the calculated strength of 36.5 ksi. Ring No. 2 had slightly different dimensions compared to No. 1 and failed at an ID burst pressure of 22.5 ksi, also considerably below its calculated burst pressure. Calculations of burst pressures did not account for the details of the degrading defects found by post-test destructive evaluation. Rings No. 1 and 2 possessed irregular fiber spacing, touching fibers, and numerous matrix cracks between fibers that could have contributed to more severe local stress-strain conditions and hence lower than expected static strength. In addition, Ring No. 2 had small regions of highly-misoriented fibers (up to 30 degrees off-axis) that appeared to be the sites of failure initiation and are suspected as being responsible for its relatively low burst strength. This unusual defect was traceable to the specific techniques utilized during manufacture that were not communicated to participants in the cooperative program. The above noted strength limiting defects, while having shown up as indications of irregularity during non-destructive evaluation, were not judged (prior to testing) as being as serious as was later determined. Since Ring No. 3 was suspected of having been compromised by similar manufacturing defects, and it was decided not to perform the originally planned cyclic loading tests.

APPLICATION OF MODEL FRAMEWORK TO PREDICTION OF RING FATIGUE LIFE

Although ring fatigue tests have as yet to be conducted, an example fatigue life prediction for postulated loading conditions is possible using the model framework presented herein. For this purpose, the dimensions and details of all three rings are utilized, resulting in the following relationship between the load per shoe, L, and the average circumfrential strain, ϵ. Thus,

$$\begin{aligned} &\text{Ring No. 1} && \epsilon = 0.000192\ L \\ &\text{Ring No. 2} && \epsilon = 0.000190\ L \\ &\text{Ring No. 3} && \epsilon = 0.000183\ L \end{aligned} \qquad (12)$$

For a cyclic loading test wherein L fluctuates between zero and a prescribed maximum value, L becomes ΔL and ϵ becomes $\Delta\epsilon$, the total strainrange. Thus, a link is established between the applied loading variable and the prime parameter, $\Delta\epsilon$, for calculating MMC fatigue life (Fig. 4).

Owing to the simple ring geometry, circumfrential orientation of the fibers, and the zero to maximum load-controlled loading, the MMC coupon specimens and the MMC material contained in the ring experience essentially identical conditions of operation. This simple fact means that the many influencing factors discussed in the section on the framework of the creep-fatigue model will affect the ring just as they would affect an MMC coupon in a laboratory test. Consequently, the laboratory generated fatigue data can be applied directly to the prediction of the fatigue life of the ring. The problem becomes trivial under these unique circumstances, and there is very little that is unique to the life prediction calculations for an MMC ring in contrast to a monolithic ring. The primary difference has to do only with the location at which failure is expected to originate.

Fatigue failure of a cyclic loaded MMC-cored ring is expected to originate at the same location that initiated static burst failure, i.e., at the inner-most diameter of the MMC core where the strainrange is 13.5% greater than the average circumfrential strainrange. Thus, the strain in the above equation must be increased by this percentage,

$$\begin{aligned} &\text{Ring No. 1} && \Delta\epsilon = 0.000218\ \Delta L \\ &\text{Ring No. 2} && \Delta\epsilon = 0.000216\ \Delta L \\ &\text{Ring No. 3} && \Delta\epsilon = 0.000208\ \Delta L \end{aligned} \qquad (13)$$

A cyclic load ΔL of 31.3 kips/shoe (average pressure applied to the ID of the rings of 22.4 ksi) gives rise to total strainranges of 0.00683, 0.00676, and 0.00650 in/in, respectively for Rings 1 to 3. Corresponding cyclic fatigue lives, determined directly from Fig. 4, are 2935, 3130, and 4000.

In calculating the predicted fatigue life, no consideration has been given to potentially important factors such as statistical distribution of fatigue lives and size effects. The volume of composited material in a ring is nearly 600 times greater than in a single fatigue test coupon. The greater volume of the rings and the greater complexity of their manufacture would certainly invite a higher probability for life degrading defects. Calibrated statistical and probabalistic models to cover these factors are currently lacking.

SUMMARY

A framework of a deterministic engineering model has been proposed for a life prediction system applicable to isothermal creep-fatigue loading of unidirectional, continuous-fiber, MMCs. A local micromechanics stress-strain approach was adopted to impart the maximum degree of generality. The classically fatigue-prone metal matrix was selected as the vehicle for tracking the cycle-dependent changes (mean stress relaxation, hardening, softening, micro-crack initiation, and micro-crack propagation). The presence of fibers and interfacial layers is taken into account by the influence they exert on the stress-strain and failure response behavior of the matrix material. Similarly, the influence on the fiber of the presence of the interfacial and matrix materials is given consideration. Considerably more analytical and experimental research is needed to expand upon the framework and bring the approach to its full potential. Examples of isothermal fatigue data for SCS-6/Ti-15-3 illustrate important aspects of the modeling framework. Projections of the approach to the calculation of radial burst strength and anticipated fatigue strength of cyclically-loaded MMC rings was also accomplished.

ACKNOWLEDGEMENT

The cooperative sharing of data by P&WA and NASA-Lewis colleagues is greatly appreciated.

REFERENCES

Arnold, S. M.; Arya, V. K.; and Melis, M. E., 1990, "Elastic/Plastic Analyses of Advanced Composites Investigating the Use of the Compliant Layer Concept in Reducing Residual Stress Resulting from Processing," NASA TM-103204, National Aeronautics and Space Administration, Washington, DC.

Bodner, S. R. and Partom, Y., 1975, "Constitutive Equations for Elastic-Viscoplastic Strain-Hardening Materials," Journal of Applied Mechanics, Vol. 42, No. 2, pp. 385-389.

Chen, E. J. H. and Young, J. C., 1991, "The Microdebonding Testing System - A Method of Quantifying Adhesion in Real Composites," Composites Science and Technology, Vol. 42, No. 1-3, pp. 189-206.

Freed, A., 1988, "Thermoviscoplastic Model With Application to Copper," NASA Report TP 2845, National Aeronautics and Space Administration, Washington, DC.

Gayda, J., Gabb, T. P., and Freed, A. D., 1990, "The Isothermal Fatigue Behavior of a Unidirectional SiC/Ti Composite and the Ti Alloy Matrix," Fundamental Relationships Between Microstructure & Mechanical Properties of Metal-Matrix Composites, P. K. Liaw and M. N. Gungor, The Minerals, Metals & Materials Society, pp. 497-514.

Ghosn, L. J., Kantzos, P., and Telesman, J., 1991, "Modeling of Crack Bridging in a Unidirectional Metal Matrix Composite," NASA TM 104355, National Aeronautics and Space Administration, Washington, DC.

Halford, G. R. and Nachtigall, A. J., 1980, "The Strainrange Partitioning Behavior of an Advanced Gas Turbine Disk Alloy, AF2-1DA," Journal of Aircraft, Vol. 17, No. 8, pp. 598-604.

Halford, G. R., Lerch, B. A., Saltsman, J. F., Arya, V., and Caruso, J. J., 1989, "LCF Life Prediction for MMCs," HITEMP Review 1989, NASA CP-10039, National Aeronautics and Space Administration, Washington, DC, pp. 64-1 to 64-9. *ITAR Restricted Document.*

Halford, G. R., Verrilli, M. J., Kalluri, S., Ritzert, F. J., Duckert, R. E., and Holland, F., 1991a, "Thermomechanical and Bithermal Fatigue Behavior of Cast B1900 + Hf and Wrought Haynes 188," Advances in Fatigue Lifetime Predictive Techniques, ASTM STP 1122, M. R. Mitchell and R. W. Landgraf, Eds., American Society for Testing and Materials, Philadelphia, pp. 120-142.

Halford, G. R., Saltsman, J. F., Verrilli, M. J., and Arya, V., 1991b, "Application of a New Thermal Fatigue Life Prediction Model to Two High-Temperature Aerospace Alloys," Advances in Fatigue Lifetime Predictive Techniques, ASTM STP 1122, M. R. Mitchell and R. W. Landgraf, Eds., American Society for Testing and Materials, Philadelphia, pp. 107-119.

Halford, G. R., Lerch, B. A., Saltsman, J. F., 1993, "Proposed Framework for Thermomechanical Life Modeling of Metal Matrix Composites," NASA TP 3320, National Aeronautics and Space Administration, Washington, DC.

Hashin, Z. and Rotem, A., 1973, "A Fatigue Failure Criterion for Fiber Reinforced Materials," Journal of Composite Materials, Vol. 7, pp. 448-464.

Jansson, S., and Leckie, F. A., 1990, "Reduction of Thermal Stresses in Continuous Fiber Reinforced Metal Matrix Composites with Interface Layers," NASA CR-185302, National Aeronautics and Space Administration, Washington, DC.

Lerch, B. A.; Gabb, T. P.; and MacKay, R. A., 1990, "Heat Treatment Study of the SiC/Ti-15-3 Composite System," NASA TP-2970, National Aeronautics and Space Administration, Washington, DC.

Manson, S. S., 1965, "Fatigue: A Complex Subject -- Some Simple Approximations," Experimental Mechanics, Vol. 5, No. 7, pp. 193-226.

Manson, S. S. and Halford, G. R., 1976, "Treatment of Multiaxial Creep-Fatigue by Strainrange Partitioning," Symposium on Creep-Fatigue Interaction, MPC-3, R. M. Curran, Ed., American Society of Mechanical Engineers and the Metals Properties Council, New York, pp. 299-322.

Manson, S. S. and Halford, G. R., 1977, "Discussion of paper by J. J. Blass and S. Y. Zamrik in Symposium on Creep-Fatigue Interaction, ASME, 1976, pp. 129-159," Journal of Engineering Materials and Technology, Vol. 99, pp. 283-286.

Morrow, J. (1968), "Fatigue Properties in Metals," Section 3.2, Fatigue Design Handbook, J. A. Graham, Ed., Society of Automotive Engineers, Inc., Warrendale, PA, pp. 21-29.

Robinson, D. A. and Swindeman, R. W., 1982, "Unified Creep-Plasticity Constitutive Equations for 2-1/4Cr-1Mo Steel at Elevated Temperature,". ORNL Report TM-8444, Oak Ridge National Laboratories, Oak Ridge, Tennessee.

Saltsman, J. F. and Halford, G. R., 1988a, "An Update on the Total Strain Version of SRP," Low Cycle Fatigue, ASTM STP 942, H. D. Solomon, G. R. Halford, L. R. Kaisand, and B. N. Leis, Eds., American Society for Testing and Materials, Philadelphia, pp. 329-341.

Saltsman, J. F. and Halford, G. R., 1988b, "Life Prediction of Thermomechanical Fatigue Using The Total Strain Version of Strainrange Partitioning (SRP)---A Proposal. NASA TP-2779, National Aeronautics and Space Administration, Washington, DC.

Walker, K. P., 1981, "Research and Development Program for Nonlinear Structural Modeling With Advanced Time-Temperature Dependent Constitutive Relations," NASA CR-165533, National Aeronautics and Space Administration, Washington, DC.